Research Paper

Circular RNA LPAR3 enhances GPX4 expression by targeting miR-196a-5p to suppress ferroptosis of osteosarcoma cells

Xian-E Cao[1], Ji-Wei Chai[1,*], Ping Li[2,*], Jun-Hong Li[3], Xi-Xia Wang[4], Fan-Bin Meng[1]

[1]Department of Orthopaedics, Linyi People's Hospital, Linyi, Shandong Province, China
[2]Department of Orthopaedics, Jinan People's Hospital Affiliated to Shandong First Medical University, Jinan, Shandong Province, China
[3]Department of Cardiology, Jinan People's Hospital Affiliated to Shandong First Medical University, Jinan, Shandong Province, China
[4]Central Sterile Supply Department, Linyi People's Hospital, Linyi, Shandong Province, China
*Equal contribution

Correspondence to: Fan-Bin Meng; **email:** fanbslyq8560@163.com
Keywords: osteosarcoma, ferroptosis, circLPAR3, miR-196a-5p, GPX4
Received: April 14, 2021 **Accepted:** July 30, 2021 **Published:**

ABSTRACT

Osteosarcoma is a prevalent bone malignancy that presents a low survival rate and high incidence of metastasis. Circular RNAs (circRNAs) have been identified as the critical regulators in osteosarcoma pathogenesis. Here, we reported an innovative function of circular RNA LPAR3 (circLPAR3) in controlling the ferroptosis of osteosarcoma cells. The expression of circLPAR3 was increased in clinical osteosarcoma samples and osteosarcoma cell lines. The proliferation and invasion/migration were repressed, but the apoptosis was induced in osteosarcoma cells by the inhibition of circLPAR3 *in vitro,* and circLPAR3 knockdown reduced the tumor growth of osteosarcoma *in vivo*. Specifically, the treatment of ferroptosis activator termed erastin suppressed the cell proliferation, and circLPAR3 shRNA further reinforced this effect in the osteosarcoma cells. Besides, the levels of iron, Fe^{2+}, and ROS were significantly increased by circLPAR3 suppression in the cells. GPX4 reconstitution could reverse circLPAR3 knockdown-induced ferroptosis of osteosarcoma cells. circLPAR3 activated GPX4 expression by sponging miR-196a-5p in the cells. MiR-196a-5p contributed to osteosarcoma cell ferroptosis by targeting GPX4. The circLPAR3 inhibition-attenuated malignant phenotypes of osteosarcoma cells were rescued by the overexpression of GPX4 or miR-196a-5p inhibitor. Consequently, we concluded that circular RNA circLPAR3 enhanced GPX4 expression through sponging miR-196a-5p to suppress ferroptosis in osteosarcoma development. CircLPAR3 and miR-196a-5p may serve as promising targets for osteosarcoma therapy.

INTRODUCTION

Osteosarcoma serves as malignant bone cancer, mainly in children and adolescents under 20 years old [1, 2]. Though therapeutic technologies, including operation and multi-drug chemotherapy, have been advanced, osteosarcoma patients' prognosis is still unsatisfactory because of metastasis and drug resistance [3, 4]. Molecular modifications in crucial signaling regulated by non-coding RNA are required for osteosarcoma development, such as metastasis, invasion, and proliferation [5, 6]. Meanwhile, ferroptosis is a recently recognized programmed cell death characterized by iron metabolism regulation and lipid peroxidation [7–9]. Glutathione peroxidase 4 (GPX4) is a significant negative regulator of ferroptosis in cancer progression [10, 11]. However, the molecular mechanism of ferroptosis regulation in osteosarcoma pathogenesis remains obscure.

Substantial human gene populations are commonly transcripts, and multiple transcripts are non-coding RNAs (ncRNAs) [12, 13]. Circular RNAs (circRNAs) are a sort of ncRNAs with a circular structure distinctive from the linear RNA [14]. CircRNAs possess various critical functions in tumorigenesis [15]. And increasing evidence indicates that circRNAs serve as miRNA sponges to regulate different gene expressions [16]. Lysophosphatidic acid (LPA) is a small lysophosphatidic molecule that modulates multiple cellular processes by regulating G-protein-coupled receptors [17]. Lysophosphatidic acid receptor 3 (LPAR3) is the receptor of LPA and has been identified as a crucial contributor to multiple cancer progression, including melanoma and thyroid cancer [18, 19]. Circular RNA LPAR3 (circLPAR3) derives from LPAR3 gene and also terms crc0004390. It has been reported that circular RNA LPAR3 has presented tumor contributor function in esophageal cancer cells by sponging miR-198 [20]. Our circRNA microarray analysis identified that circLPAR3 expression was elevated in clinical osteosarcoma samples. Meanwhile, previous studies have identified that miR-196a-5p is involved in circular RNAs-mediated cancer progression in cervical cancer and oral squamous cell carcinoma [21, 22]. However, association of circLPAR3 with miR-196a-5p in osteosarcoma is still obscure.

Here, we tried to determine the function and mechanism of circLPAR3 in controlling the ferroptosis of osteosarcoma cells. We found that circLPAR3 promoted GPX4 expression through sponging miR-196a-5p to suppress ferroptosis in osteosarcoma development.

RESULTS

CircLPAR3 inhibition represses osteosarcoma cell viability and invasion/migration but enhances apoptosis

To identify the potential circular RNAs which are involved in the modulation of osteosarcoma progression, we performed the circular RNA microarray analysis in clinical osteosarcoma samples and primary chondroma samples. Among the differently expressed circular RNAs, we identified that circLPAR3 presented a most significant elevation in the osteosarcoma samples (Figure 1A). Our data validated that the expression of circLPAR3 was enhanced in the clinical osteosarcoma tissues (n=50) and osteosarcoma cell lines (Figure 1B, 1C). We treated the U2OS and MG63 cells with LPAR3 shRNA and found that circLPAR3 expression remarkably down-regulated in the cells (Figure 1D). Functionally, the cell proliferation was repressed by circLPAR3 knockdown in the U2OS and MG63 cells (Figure 1E). Conversely, apoptosis was enhanced by circLPAR3 shRNA in the cells (Figure 1F, 1G). Impressively, the depletion of circLPAR3 attenuated the invasion/migration of U2OS and MG63 cell lines (Figure 1H, 1I).

CircLPAR3 knockdown promotes osteosarcoma cells ferroptosis

We then were interested in the function of circLPAR3 in ferroptosis of osteosarcoma cells. The treatment of ferroptosis stimulator termed erastin reduced the cell proliferation relative to DMSO, and circLPAR3 shRNA further reinforced this effect (Figure 2A, 2B). But we failed to observe the significant effect of circLPAR3 shRNA on the ferroptosis inhibitor called ferrostatin-1 (Figure 2A, 2B). In addition, the levels of iron, Fe^{2+}, and ROS were significantly increased by circLPAR3 suppression in osteosarcoma cells (Figure 2C–2E).

GPX4 participates in circLPAR3-regulated ferroptosis in osteosarcoma cells

We then explored the potential mechanisms of circLPAR3-mediated ferroptosis. Given that SLC7A11 and GPX4 are the essential regulators and the molecular markers of ferroptosis, we were interested in whether circLPAR3 modulates SLC7A11 and GPX4 expression in the regulation of ferroptosis of osteosarcoma. Significantly, we found that the protein expression of SLC7A11 and GPX4 was repressed by circLPAR3 shRNA, in which the re-introduction of GPX4 rescued the expression of these factors in osteosarcoma cells (Figure 3A). Moreover, the accumulation of iron, Fe^{2+}, and ROS was induced by circLPAR3 depletion, and the overexpression of GPX4 could attenuate this phenotype in osteosarcoma cells (Figure 3B–3D). We then validated that SLC7A11 and GPX4 were enhanced in clinical osteosarcoma tissues (n=50) (Figure 3E, 3F). We then selected GPX4 for the further analysis.

CircLPAR3 activates GPX4 expression by targeting miR-196a-5p

To determine the potential mechanism of circLPAR3 modulating GPX4 expression, we evaluated the potential interacted miRNAs with circLPAR3 and GPX4 using ENCORI database. In the potential miRNAs that both interacted with circLPAR3 and GPX4, RNA-pull down analysis identified that miR-196a-5p presented the highest interaction enrichment with circLPAR3 in U2OS cells (Figure 4A). We

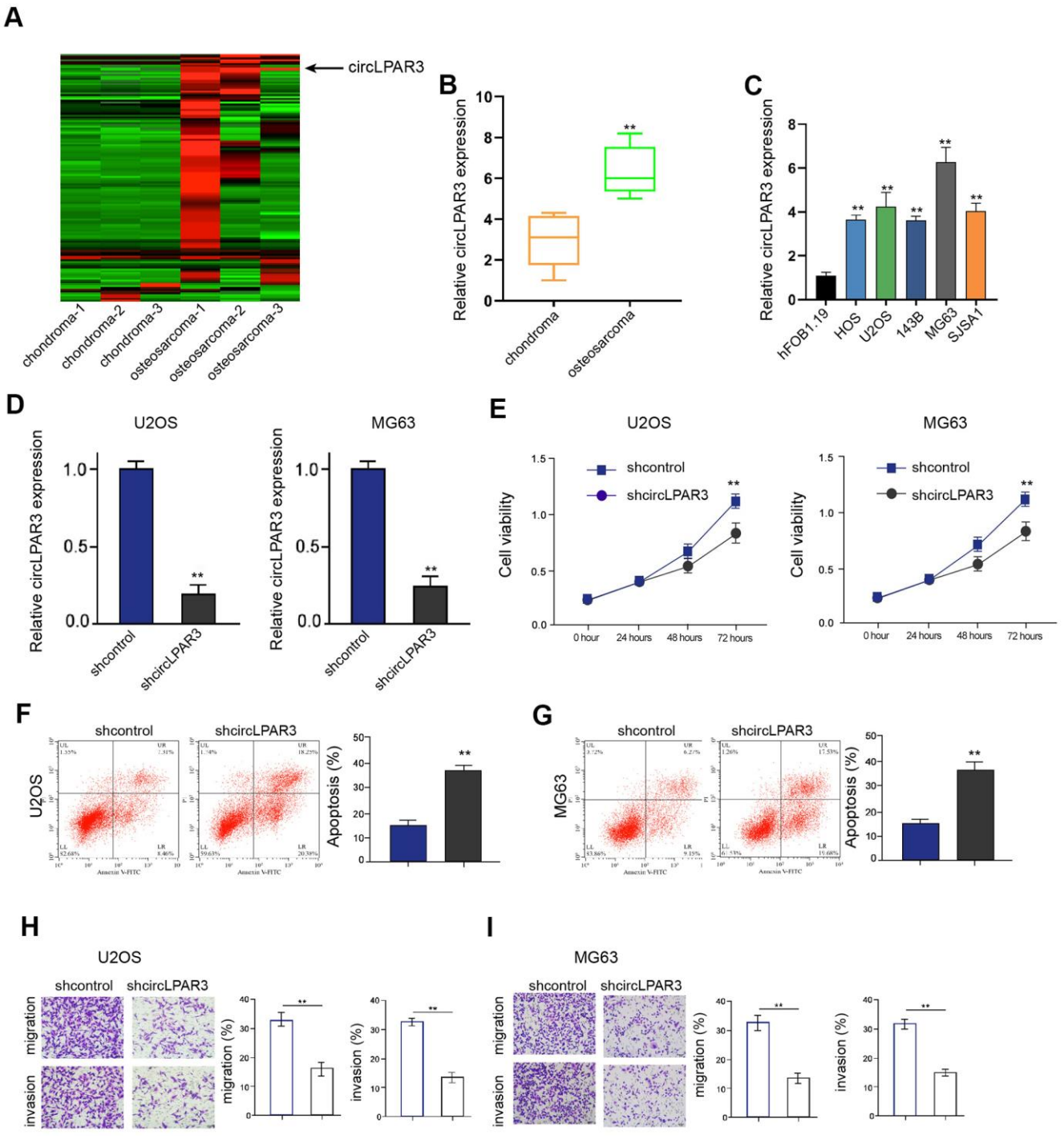

Figure 1. CircLPAR3 inhibition represses proliferation, invasion and migration but enhances apoptosis of osteosarcoma cells. (**A**) Heat map and hierarchical clustering analysis of circRNAs which were differentially expressed between clinical osteosarcoma samples (n=3) and primary chondroma samples (n=3) in circular RNA microarray analysis. Each column represented the expression profile of a tissue sample), and each row corresponds to a circRNA (log foldchange (FC) ≥ 2 and $P < 0.05$). Red color represented up-regulated circRNAs, and green color represented down-regulated circRNAs. (**B**) The expression of circLPAR3 was detected in clinical osteosarcoma samples (n=50) by qPCR. (**C**) The expression of circLPAR3 was determined by qPCR in hFOB1.19 cell line and osteosarcoma cell lines, including HOS, U2OS, 143B, MG63, and SJSA1. (**D**–**I**) The functional analysis was performed in the U2OS and MG63 cells treated with control shRNA (shcontrol) or circLPAR3 shRNA. (**D**) The expression of circLPAR3 was measured by qPCR in the cells. (**E**) The cell viability of U2OS and MG63 cells was analyzed by MTT assays. (**F**, **G**) The apoptosis of U2OS and MG63 cells was assessed by flow cytometry analysis. (**H**, **I**) The invasion and migration of U2OS and MG63 cells were detected by transwell assays. ** $P < 0.01$.

confirmed the interaction of miR-196a-5p with circLPAR3 and GPX4 mRNA 3'UTR (Figure 4B). The miR-196a-5p mimic notably enhanced its expression in the osteosarcoma cells (Figure 4C). MiR-196a-5p attenuated luciferase activities of both circLPAR3 and GPX4 mRNA 3'UTR in osteosarcoma cells (Figure 4D, 4E). The circLPAR3 shRNA induced miR-196a-5p expression and miR-196a-5p mimic suppressed GPX4 expression in osteosarcoma cells (Figure 4F, 4G). Significantly, the GPX4 levels were alleviated followed by circLPAR3 inhibition but miR-196a-5p inhibitor could reverse this effect in the U2OS and MG63 cells (Figure 4H). Then, we validated that miR-196a-5p expression was reduced in clinical osteosarcoma tissues (n=50) and negatively correlated with GPX4 expression in the tissues (Figure 4I, 4J).

MiR-196a-5p contributes to osteosarcoma cell ferroptosis involving GPX4

Furthermore, we detected influence of miR-196a-5p/GPX4 on ferroptosis of osteosarcoma cells. Our data demonstrated that miR-196a-5p mimic reinforced the inhibitory effect of erastin on U2OS and MG63 cell proliferation, which was rescued by GPX4 overexpression (Figure 5A, 5B). Moreover, the accumulation of iron, Fe^{2+}, and ROS was induced by miR-196a-5p mimic depletion, and the re-introduction of GPX4 could attenuate this phenotype in osteosarcoma cells (Figure 5C–5E).

CircLPAR3*/miR-196a-5p/GPX4 axis is involved in regulating tumor growth *in vivo

We then observed that the inhibition of circLPAR3 attenuated the tumor size, tumor weight, and tumor volume in the tumorigenicity analysis of nude mice (Figure 6A–6C). Moreover, miR-196a-5p expression was induced but GPX4 levels were reduced in the circLPAR3 knockdown group (Figure 6D, 6E). The levels of lipid ROS and iron were induced by circLPAR3 depletion in the mice (Figure 6F, 6G).

We then identified that miR-196a-5p attenuated the tumor size/weight/volume in the tumorigenicity analysis of nude mice (Supplementary Figure 1A–1C).

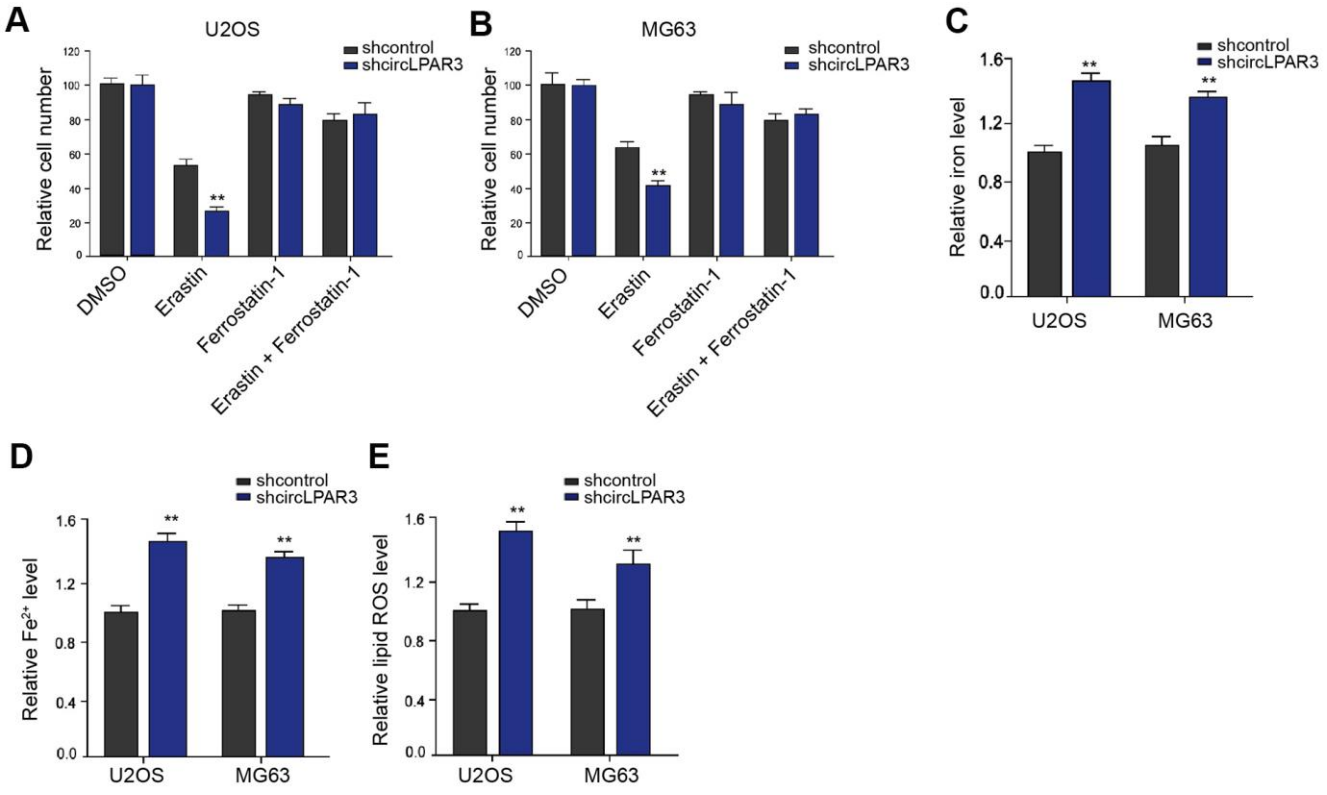

Figure 2. CircLPAR3 knockdown promotes ferroptosis of osteosarcoma cells. (**A**, **B**) The cell viability was analyzed by MTT assays in U2OS and MG63 cells co-treated with circLPAR3 shRNA and erastin (5 mmol/L) or ferrostatin (1 mmol/L). (**C**–**E**) The analysis was performed in the U2OS and MG63 cells treated with circLPAR3 shRNA. The levels of iron (**C**), Fe^{2+} (**D**), and lipid ROS (**E**) were analyzed by the corresponding measurement kits. ** $P < 0.01$.

The enhanced miR-196a-5p expression was validated in the tumor tissues of the mice (Supplementary Figure 1D). Meanwhile, the GPX4 levels were inhibited by miR-196a-5p mimic in the tumor tissues of the mice (Supplementary Figure 1E).

DISCUSSION

There are just some clues of the function of ferroptosis during osteosarcoma development. The inhibition of Nrf2/GPx4 signaling induces ferroptosis to enhance the cisplatin sensitivity in osteosarcoma

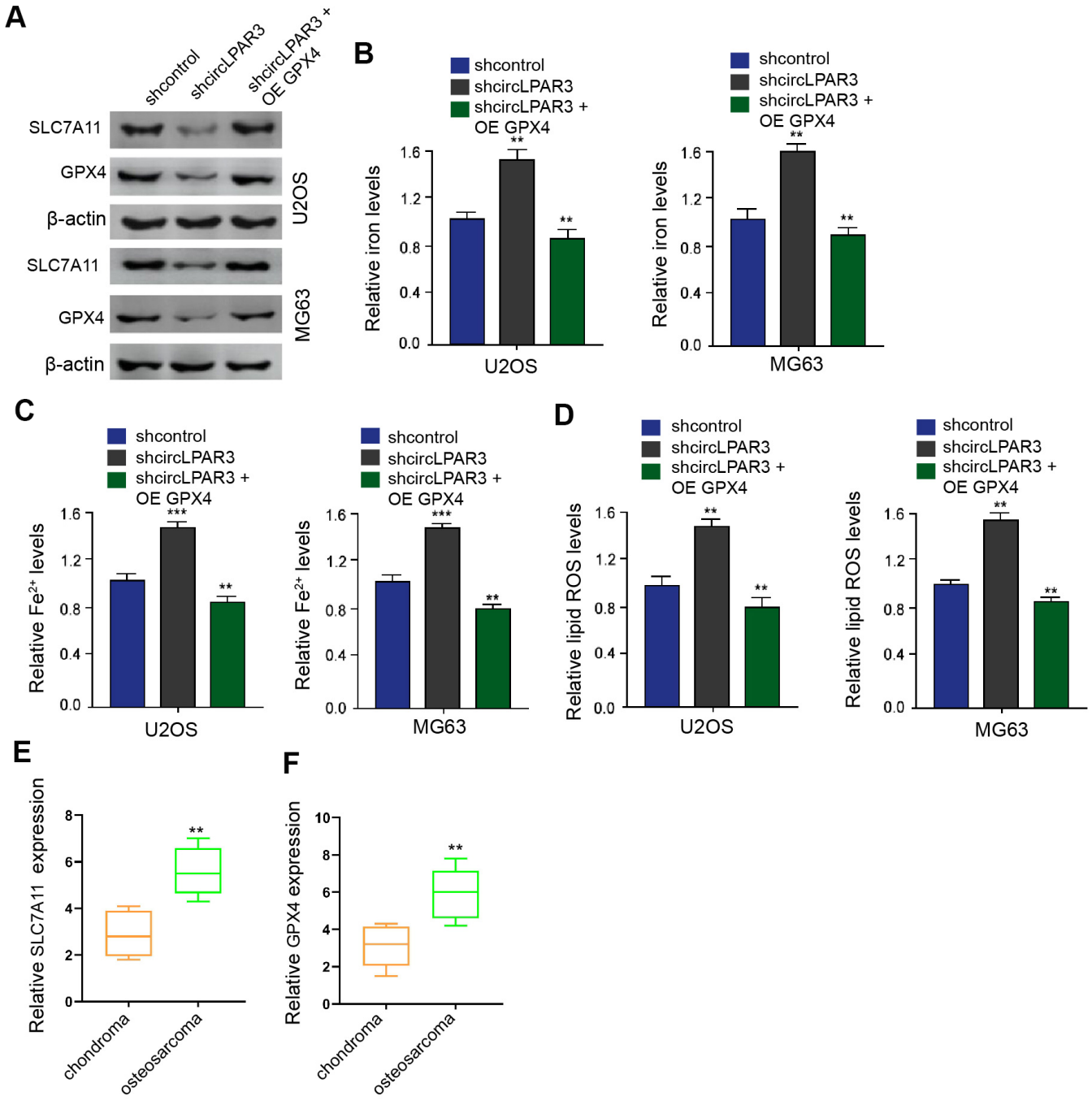

Figure 3. GPX4 participates in CircLPAR3-regulated ferroptosis in osteosarcoma cells. (**A**–**D**) The analysis was performed in the U2OS and MG63 cells treated with circLPAR3 shRNA and GPX4 reconstituted plasmid. (**A**) Western blot detected the GPX4 and SLC7A11 expression. The levels of iron (**B**), Fe^{2+} (**C**), and lipid ROS (**D**) were analyzed by the corresponding measurement kits. (**E**) The expression of SLC7A11 was measured in clinical osteosarcoma samples (n=50) by qPCR. (**F**) The expression of GPX4 was detected in clinical osteosarcoma samples (n=50) by qPCR. ** $P < 0.01$.

cells [23]. EF24 contributes to ferroptosis by modulating HMOX1 in osteosarcoma cells [24]. β-Phenethyl Isothiocyanate regulates ferroptosis by stimulating MAPK signaling and modulating iron metabolism in osteosarcoma [25]. Moreover, a lot of circular RNAs are involved in the regulation of osteosarcoma. CircTADA2A enhances metastasis and progression of osteosarcoma by promoting CREB3 expression through sponging miR-203a-3p [26]. Circ_001621 contributes to migration and proliferation by targeting miR-578 /VEGF signaling in osteosarcoma cells [27]. Circular RNA 0001785 serves as a ceRNA of miR-1200 and up-regulates HOXB2 expression to modulate the tumorigenesis of osteosarcoma [28]. Meanwhile, circular RNA LPAR3 has been identified to participate in facilitating cancer progression. Circular RNA LPAR3 facilitates metastasis, invasion, and migration of esophageal cancer cells by sponging miR-198 [20]. We showed that circLPAR3 inhibition repressed malignant phenotypes of osteosarcoma cells. CircLPAR3 knockdown promoted ferroptosis of osteosarcoma cells. Our data not only provide evidence of the novel function of circLPAR3 in osteosarcoma progression, but also elucidate the innovative role of circLPAR3 in regulating ferroptosis.

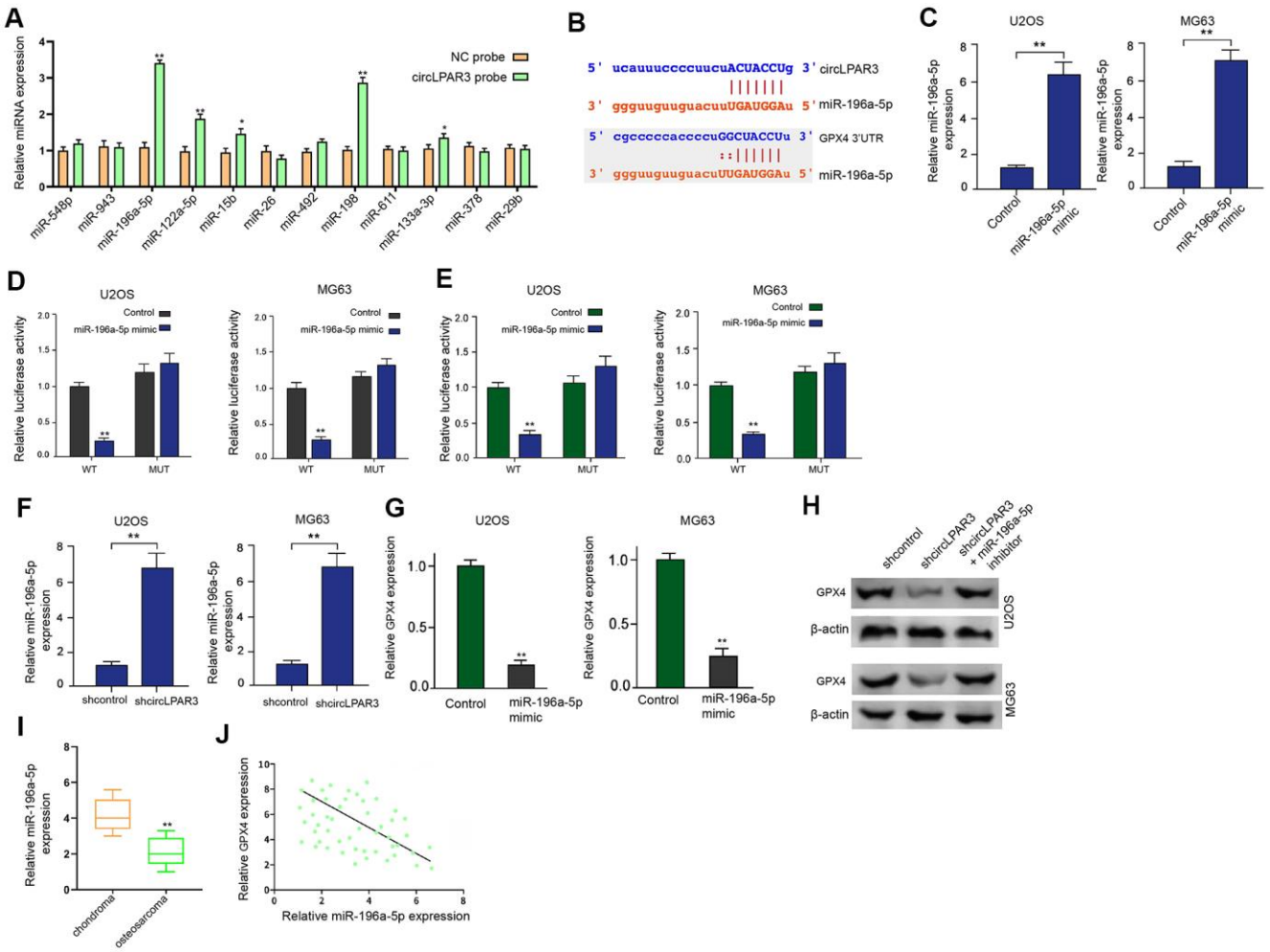

Figure 4. CircLPAR3 activates GPX4 expression by targeting miR-196a-5p. (**A**) The interaction of circLPAR3 with miRNAs was analyzed by RNA-pull down assays in U2OS cells. (**B**) The prediction analysis using ENCORI database assessed the interaction of miR-196a-5p with circLPAR3 and GPX4 mRNA 3'UTR. (**C–E**) The analysis was performed in the U2OS and MG63 cells treated with miR-196a-5p mimic. (**C**) The qPCR measured the miR-196a-5p expression. (**D**, **E**) The luciferase reporter gene assays analyzed luciferase activities of circLPAR3 and GPX4 mRNA 3'UTR. (**F**) The qPCR measured the miR-196a-5p expression in the U2OS and MG63 cells treated with circLPAR3 shRNA. (**G**) Western blot detected the GPX4 expression in the U2OS and MG63 cells treated with miR-196a-5p mimic. (**H**) Western blot tested GPX4 expression in the U2OS and MG63 cells co-treated with circLPAR3 shRNA and miR-196a-5p inhibitor. (**I**) The expression of miR-196a-5p was detected in clinical osteosarcoma samples (n=50) by qPCR. (**J**) The correlation of miR-196a-5p expression with GPX4 expression was analyzed by qPCR in clinical osteosarcoma samples (n=50). * $P < 0.05$, ** $P < 0.01$.

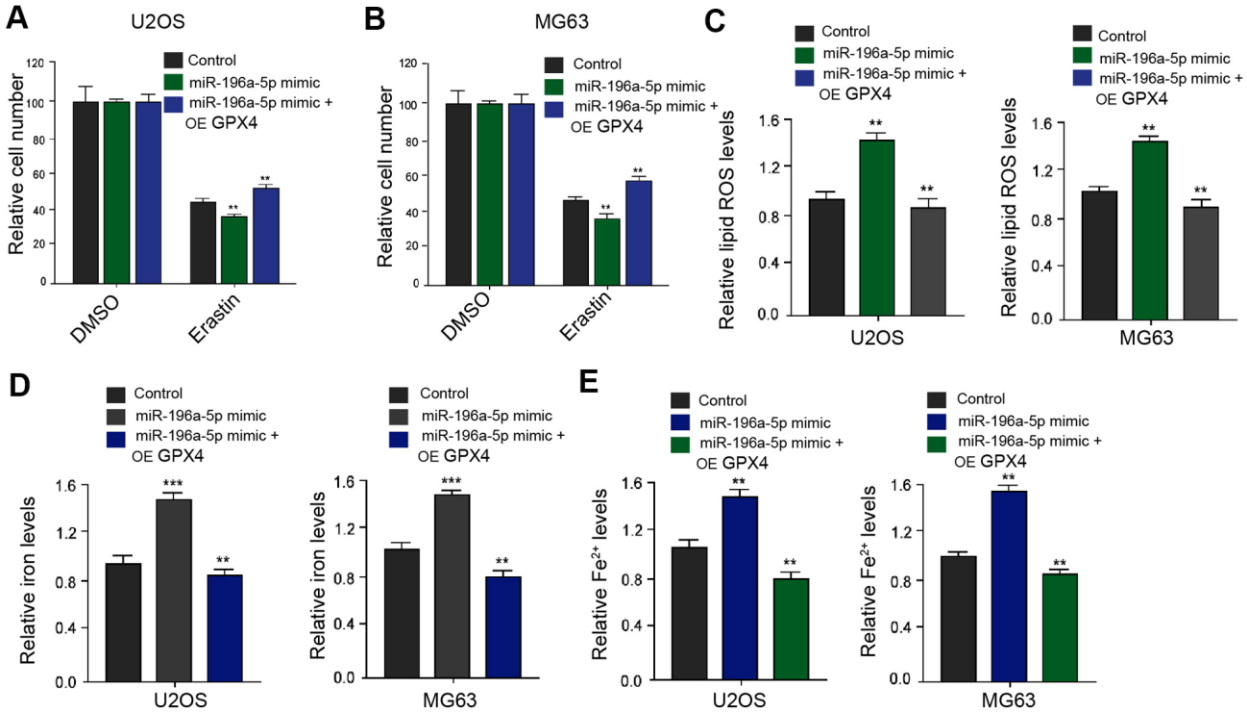

Figure 5. MiR-196a-5p contributes to osteosarcoma cell ferroptosis involving GPX4. (**A**, **B**) MTT assays analyzed cell viability in the U2OS and MG63 cells co-treated with miR-196a-5p mimic and erastin (5 mmol/L) or DMSO. (**C**–**E**) The analysis was performed in the U2OS and MG63 cells treated with miR-196a-5p mimic. The levels of iron (**C**), Fe^{2+} (**D**), and lipid ROS (**E**) were analyzed by the corresponding measurement kits. ** $P < 0.01$.

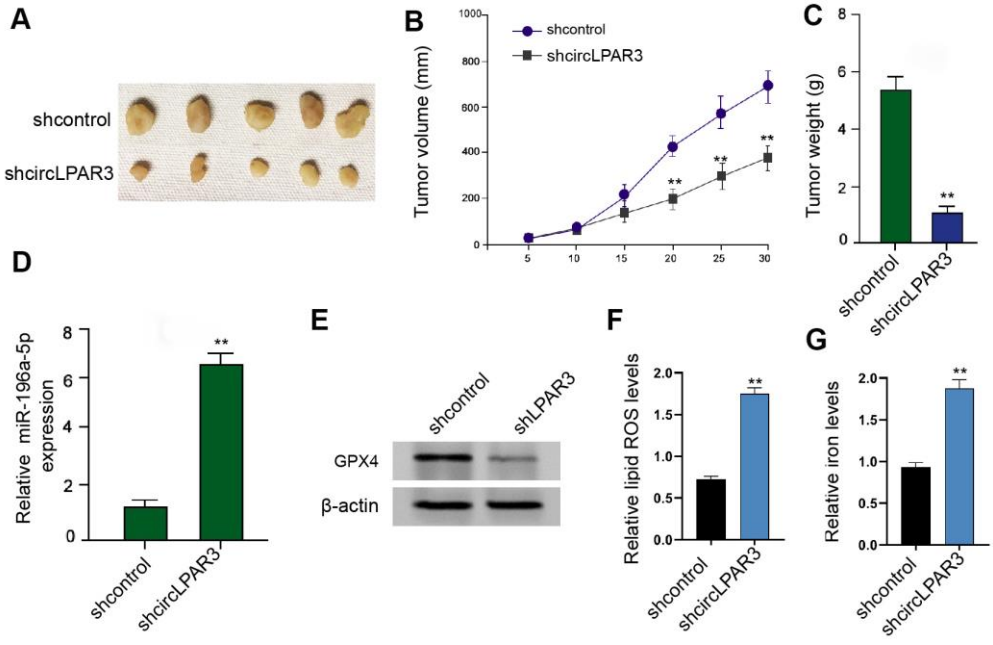

Figure 6. CircLPAR3/miR-196a-5p/GPX4 axis is involved in regulating tumor growth *in vivo*. (**A**–**E**) Tumorigenicity assay in the nude mice (n = 5) analyzed the tumor growth of U2OS cells treated with control shRNA (shcontrol) or circLPAR3 shRNA. The tumor images (**A**), tumor volume (**B**), and weight (**C**) were presented. (**D**) The qPCR detected miR-196a-5p expression in the tumor tissues. (**E**) Western blot analysis determined GPX4 expression in the tumor tissues. The levels of lipid ROS (**F**) and iron (**G**) were analyzed by the corresponding measurement kits. ** $P < 0.01$.

Previous investigations have widely demonstrated the function of miRNAs in osteosarcoma. MiRNA-206 inhibits osteosarcoma metastasis by repressing Notch3 [29]. MiRNA-552 enhances osteosarcoma cell invasion and migration by down-regulating TIMP2 [30]. MiR-422a reduces proliferation of osteosarcoma cells via the inhibition of KRAS and BCL2L2 [31]. MiR-188-5p suppresses osteosarcoma progression by targeting CCNT2 [32]. MiR-139-5p attenuates invasion and proliferation of osteosarcoma cells by targeting DNMT1 [33]. Here, we found that circLPAR3 induced GPX4 expression by targeting miR-196a-5p, regulating the malignant progression and ferroptosis of osteosarcoma cells. It indicates the significant correlation of miR-196a-5p with circLPAR3 and GPX4 in tumorigenesis. In the presented study, we identified that circLPAR3 repressed ferroptosis of osteosarcoma cells by targeting miR-196a-5p/GPX4 signaling. MiR-196a-5p/GPX4 signaling may be just one of the downstream mechanisms of circLPAR3-mediated ferroptosis of osteosarcoma cells. And more signaling pathways in which the circular RNA LPAR3 may function will be explored in future investigations.

We concluded that circular RNA LPAR3 enhanced GPX4 expression through sponging miR-196a-5p to suppress ferroptosis in osteosarcoma development. The clinical significance of circLPAR3 and miR-196a-5p in osteosarcoma therapy is deserved further investigation.

MATERIALS AND METHODS

Cell culture

The hFOB1.19 and osteosarcoma 143B, HOS, SJSA-1, U2OS, and MG63, cell lines were bought (American Type Tissue Culture Collection, ATCC). The cells were cultured at a condition of 37° C with 5% CO_2 in DMEM (BI, USA) with fetal bovine serum (10%, BI, USA), penicillin (100 units/mL, BI, USA), streptomycin (0.1 mg/mL, BI, USA). The miR-196a-5p mimic/inhibitor, circLPAR3 shRNA, and pcDNA3.1-GPX4 vector were obtained (QingKe, China).

Osteosarcoma samples

Primary chondroma and osteosarcoma tissues were collected from 50 patients before the neo-adjuvant chemotherapy. The patients were histologically characterized by a pathologist using the criteria (World Health Organization). The application of the samples was underwritten informed consent of the patients, were approved by the Ethics Committee of Linyi People's Hospital.

Circular RNA microarray analysis

The circular RNA microarray analysis was performed to explore the potential correlation of circular RNAs with osteosarcoma (BGI, China). Total RNA was obtained from 3 chondroma and osteosarcoma tissues, and linear RNAs were removed by RNase R digestion. After that, the enriched circRNAs were augmented and transcribed in fluorescent cRNAs, and analyzed by Arraystar Human circRNA Array (8 × 15K; Arraystar). The Agilent scanner G2505C scanned the microarray, the collected images were analyzed through the Agilent feature extraction software (11.0.0.1 version), and the obtained data were analyzed.

Apoptosis analysis

To detect apoptosis, U2OS and MG63 cells were treated with FITC-Annexin V/PI apoptosis kit (Beyotime). Briefly, cells were treated with FITC-Annexin V and PI (5 μl) for 30 minutes in dark, resuspended in PBS and subjected to flow cytometry (BD Bioscience).

MTT assays

Cells were seeded in a 96-well plate (2×10^4/well) after transfection with indicated vectors and/or oligonucleotides. The cells were then exposed to MTT reagent (5 mg/mL) for four hours in the standard culture incubator. The absorbance values at 570nm were measured by a micro plate reader (Bio-Rad, USA).

Luciferase reporter gene assay

The wild-type (WT) or mutant (MUT) circLPAR3 or 3'UTR of GPX4 sequences were synthesized and inserted into pmirGLO vectors. Cells were plated in a 24-well plate, and were transfected with miR-196a-5p mimics or negative control, along with the WT or MUT vectors for 48 hours. A Dual-Luciferase Reporter Assay System (Promega, USA) was adopted to detect the luciferase activity.

ROS and iron levels measurement

The reactive oxygen species (ROS) and iron analysis were performed as the previous report [34]. The ROS levels were detected by DCFH-DA staining. The levels of iron and Fe2+ were analyzed by Iron Assay Kit in the cells.

Transwell assays

The invasion/migration of U2OS and MG63 cells was analyzed by using transwell chambers (Corning, USA).

U2OS and MG63 cells were plated in the upper chamber with FBS-free DMEM medium. The lower chambers were filled with DMEM for 48 hours. The upper chamber was treated with paraformaldehyde (4%), dyed by crystal violet (0.1%) for 20 minutes, followed by the photograph and counting using a microscope. To detect cell invasion, the upper chambers were covered by Matrigel (BD Bioscience, USA).

RNA pulldown

Biotin-labeled circLPAR3 were synthesized by QIAGENE, and transfected to U2OS cells for 48 hours. The cells were then lysed and hatched with magnetic beads (Thermo) for 3 hours, followed by washing and detection by real-time PCR to measure the level of miRNAs.

Western blot analysis

Mice tissues or cells were homogenized by RIPA lysis buffer (Thermo). Proteins (30μg) were divided on SDS-polyacrylamide gel (SDS-PAGE), blotted onto polyvinylidene difluoride (PVDF) membranes. After that, the blots were blocked by 5% skim milk in PBST, incubated with specific primary antibodies against GPX4 (1:1000, Abcam, USA), SLC7A11 (1:1000, Abcam, USA), and β-actin (1:1000, Abcam, USA) at 4° C overnight. The blots were then hatched with secondary anti-rabbit or anti-mouse IgG conjugated with horse radish peroxidase (HRP) (Abcam, USA) at room temperature for 1 hour. The blots were then infiltrated with ECL (Thermo) and visualized in a Gel image system.

Quantitative reverse transcription-PCR (qRT-PCR)

The total RNA was extracted with Trizol reagent (Thermo) following a standard protocol. The cDNA was synthesized by using a PrimeScript™ 1st Strand cDNA Synthesis Kit (TaKaRa, Dalian, China). Quantitative real time PCR was conducted with Power Up SYBR Green Master Mix (Applied Biosystem, USA). Data were calculated by the $2^{-\Delta\Delta Ct}$ methods with GAPDH and U6 as reference genes, respectively. Primers were listed: GPX4: sense, 5′-GAGGCAAGACCGAAGTAAACTAC -3′, antisense, 5′-CCGAACTGGTTACACGGGAA -3′; miR-196a-5p: sense, 5′-CCGACGTAGGTAGTTTCATGTT -3′, antisense, 5′-GTGCAGGGTCCGAGGTATTC-3′; circLPAR3: sense, 5′-GAGTTACCTTGTTTTCTGGA CA-3′, antisense: 5′-TGGAGAAGTGAACATCCTAAG-3′; GAPDH: sense, 5′-CATGGGTGTGAACCATGAGA-3′, antisense, 5′-CAGTGATGGCATGGACTG-TG-3′; U6: sense, 5′-CGCGCTTCGGCAGCACATATACT-3′, antisense, 5′-ACGCTTCACGAATTTGCGTGTC-3′.

Analysis of tumorigenicity in nude mice

ALL animal experiments in this work were conducted under the approval of Ethics Committee of the the Animal Ethics Committee of Linyi People's Hospital. Balb/c nude mice (4-weeks old) were ordered from Vital River Laboratory (China) and fed in a SPF environment. The mice were randomly divided into two groups, then U2OS cells (1×10^7/mouse) were hypodermically injected in the nude mice. Tumor volume was analyzed by width $(mm)^2$ × length (mm)/2.

Statistical analysis

Data were shown by means ± standard deviation. Student's *t* test or one-way analysis of variance with Dunnett's multiple comparisons test were applied for comparison between two or multiple groups. $P < 0.05$ were statistically significant.

AUTHOR CONTRIBUTIONS

Xian-E Cao and Ji-Wei Chai designed the experiments. Ping-Li and Jun-Hong Li performed the experiments and analysed the data. Xi-Xia Wang performed analysis. Fan-Bin Meng wrote the paper.

CONFLICTS OF INTEREST

The authors declare that they have no conflicts of interest.

REFERENCES

1. Li Z, Shen J, Chan MT, Wu WK. The long non-coding RNA SPRY4-IT1: An emerging player in tumorigenesis and osteosarcoma. Cell Prolif. 2018; 51:e12446. https://doi.org/10.1111/cpr.12446 PMID:29484753

2. Li Z, Xu D, Chen X, Li S, Chan MT, Wu WK. LINC01133: an emerging tumor-associated long non-coding RNA in tumor and osteosarcoma. Environ Sci Pollut Res Int. 2020; 27:32467–73. https://doi.org/10.1007/s11356-020-09631-1 PMID:32556990

3. Wang C, Jing J, Cheng L. Emerging roles of non-coding RNAs in the pathogenesis, diagnosis and prognosis of osteosarcoma. Invest New Drugs. 2018; 36:1116–32. https://doi.org/10.1007/s10637-018-0624-7 PMID:30079443

4. Wang C, Ren M, Zhao X, Wang A, Wang J. Emerging Roles of Circular RNAs in Osteosarcoma. Med Sci Monit. 2018; 24:7043–50.

https://doi.org/10.12659/MSM.912092
PMID:30282962

5. Wang J, Liu S, Shi J, Li J, Wang S, Liu H, Zhao S, Duan K, Pan X, Yi Z. The Role of miRNA in the Diagnosis, Prognosis, and Treatment of Osteosarcoma. Cancer Biother Radiopharm. 2019; 34:605–13. https://doi.org/10.1089/cbr.2019.2939 PMID:31674804

6. Zhang Y, Li J, Wang Y, Jing J, Li J. The Roles of Circular RNAs in Osteosarcoma. Med Sci Monit. 2019; 25:6378–82. https://doi.org/10.12659/MSM.915559 PMID:31446435

7. Koren E, Fuchs Y. Modes of Regulated Cell Death in Cancer. Cancer Discov. 2021; 11:245–65. https://doi.org/10.1158/2159-8290.CD-20-0789 PMID:33462123

8. Liu J, Zhang C, Wang J, Hu W, Feng Z. The Regulation of Ferroptosis by Tumor Suppressor p53 and its Pathway. Int J Mol Sci. 2020; 21:8387. https://doi.org/10.3390/ijms21218387 PMID:33182266

9. Tang D, Chen X, Kang R, Kroemer G. Ferroptosis: molecular mechanisms and health implications. Cell Res. 2021; 31:107–25. https://doi.org/10.1038/s41422-020-00441-1 PMID:33268902

10. Chen X, Kang R, Kroemer G, Tang D. Broadening horizons: the role of ferroptosis in cancer. Nat Rev Clin Oncol. 2021; 18:280–96. https://doi.org/10.1038/s41571-020-00462-0 PMID:33514910

11. Chen X, Yu C, Kang R, Kroemer G, Tang D. Cellular degradation systems in ferroptosis. Cell Death Differ. 2021; 28:1135–48. https://doi.org/10.1038/s41418-020-00728-1 PMID:33462411

12. Wang S, Zhang K, Tan S, Xin J, Yuan Q, Xu H, Xu X, Liang Q, Christiani DC, Wang M, Liu L, Du M. Circular RNAs in body fluids as cancer biomarkers: the new frontier of liquid biopsies. Mol Cancer. 2021; 20:13. https://doi.org/10.1186/s12943-020-01298-z PMID:33430880

13. Wang X, Li H, Lu Y, Cheng L. Circular RNAs in Human Cancer. Front Oncol. 2021; 10:577118. https://doi.org/10.3389/fonc.2020.577118 PMID:33537235

14. Wei G, Zhu J, Hu HB, Liu JQ. Circular RNAs: Promising biomarkers for cancer diagnosis and prognosis. Gene. 2021; 771:145365. https://doi.org/10.1016/j.gene.2020.145365 PMID:33346098

15. Yang Q, Li F, He AT, Yang BB. Circular RNAs: Expression, localization, and therapeutic potentials. Mol Ther. 2021; 29:1683–702. https://doi.org/10.1016/j.ymthe.2021.01.018 PMID:33484969

16. Zhou WY, Cai ZR, Liu J, Wang DS, Ju HQ, Xu RH. Circular RNA: metabolism, functions and interactions with proteins. Mol Cancer. 2020; 19:172. https://doi.org/10.1186/s12943-020-01286-3 PMID:33317550

17. Lin YN, Audira G, Malhotra N, Ngoc Anh NT, Siregar P, Lu JH, Lee H, Hsiao CD. A Novel Function of the Lysophosphatidic Acid Receptor 3 (LPAR3) Gene in Zebrafish on Modulating Anxiety, Circadian Rhythm Locomotor Activity, and Short-Term Memory. Int J Mol Sci. 2020; 21:2837. https://doi.org/10.3390/ijms21082837 PMID:32325720

18. Byrnes CC, Jia W, Alshamrani AA, Kuppa SS, Murph MM. miR-122-5p Expression and Secretion in Melanoma Cells Is Amplified by the LPAR3 SH3-Binding Domain to Regulate Wnt1. Mol Cancer Res. 2019; 17:299–309. https://doi.org/10.1158/1541-7786.MCR-18-0460 PMID:30266753

19. Xia W, Jie W. ZEB1-AS1/miR-133a-3p/LPAR3/EGFR axis promotes the progression of thyroid cancer by regulating PI3K/AKT/mTOR pathway. Cancer Cell Int. 2020; 20:94. https://doi.org/10.1186/s12935-020-1098-1 PMID:32231464

20. Shi Y, Fang N, Li Y, Guo Z, Jiang W, He Y, Ma Z, Chen Y. Circular RNA LPAR3 sponges microRNA-198 to facilitate esophageal cancer migration, invasion, and metastasis. Cancer Sci. 2020; 111:2824–36. https://doi.org/10.1111/cas.14511 PMID:32495982

21. Jiao J, Jiao X, Liu Q, Qu W, Ma D, Zhang Y, Cui B. The Regulatory Role of circRNA_101308 in Cervical Cancer and the Prediction of Its Mechanism. Cancer Manag Res. 2020; 12:4807–15. https://doi.org/10.2147/CMAR.S242615 PMID:32606970

22. Wang L, Wei Y, Yan Y, Wang H, Yang J, Zheng Z, Zha J, Bo P, Tang Y, Guo X, Chen W, Zhu X, Ge L. CircDOCK1 suppresses cell apoptosis via inhibition of miR-196a-5p by targeting BIRC3 in OSCC. Oncol Rep. 2018; 39: 951–66. https://doi.org/10.3892/or.2017.6174 PMID:29286141

23. Liu Q, Wang K. The induction of ferroptosis by impairing STAT3/Nrf2/GPx4 signaling enhances the

sensitivity of osteosarcoma cells to cisplatin. Cell Biol Int. 2019; 43:1245–56.
https://doi.org/10.1002/cbin.11121
PMID:30811078

24. Lin H, Chen X, Zhang C, Yang T, Deng Z, Song Y, Huang L, Li F, Li Q, Lin S, Jin D. EF24 induces ferroptosis in osteosarcoma cells through HMOX1. Biomed Pharmacother. 2021; 136:111202.
https://doi.org/10.1016/j.biopha.2020.111202
PMID:33453607

25. Lv H, Zhen C, Liu J, Shang P. β-Phenethyl Isothiocyanate Induces Cell Death in Human Osteosarcoma through Altering Iron Metabolism, Disturbing the Redox Balance, and Activating the MAPK Signaling Pathway. Oxid Med Cell Longev. 2020; 2020:5021983.
https://doi.org/10.1155/2020/5021983
PMID:32322335

26. Wu Y, Xie Z, Chen J, Chen J, Ni W, Ma Y, Huang K, Wang G, Wang J, Ma J, Shen S, Fan S. Circular RNA circTADA2A promotes osteosarcoma progression and metastasis by sponging miR-203a-3p and regulating CREB3 expression. Mol Cancer. 2019; 18:73.
https://doi.org/10.1186/s12943-019-1007-1
PMID:30940151

27. Ji X, Shan L, Shen P, He M. Circular RNA circ_001621 promotes osteosarcoma cells proliferation and migration by sponging miR-578 and regulating VEGF expression. Cell Death Dis. 2020; 11:18.
https://doi.org/10.1038/s41419-019-2204-y
PMID:31907361

28. Li S, Pei Y, Wang W, Liu F, Zheng K, Zhang X. Circular RNA 0001785 regulates the pathogenesis of osteosarcoma as a ceRNA by sponging miR-1200 to upregulate HOXB2. Cell Cycle. 2019; 18:1281–91.
https://doi.org/10.1080/15384101.2019.1618127
PMID:31116090

29. Cai WT, Guan P, Lin MX, Fu B, Wu B, Wu J. MiRNA-206 suppresses the metastasis of osteosarcoma via targeting Notch3. J Biol Regul Homeost Agents. 2020; 34:775–83.
https://doi.org/10.23812/20-72-A-26 PMID:32627519

30. Chao Y, Hu K, Wang X, Wang L. MicroRNA-552 promotes migration and invasion of osteosarcoma through targeting TIMP2. Biochem Biophys Res Commun. 2019; 511:63–68.
https://doi.org/10.1016/j.bbrc.2019.02.007
PMID:30765222

31. Zhang H, He QY, Wang GC, Tong DK, Wang RK, Ding WB, Li C, Wei Q, Ding C, Liu PZ, Cui HC, Zhang X, Li D, et al. miR-422a inhibits osteosarcoma proliferation by targeting BCL2L2 and KRAS. Biosci Rep. 2018; 38:BSR20170339.
https://doi.org/10.1042/BSR20170339
PMID:29358307

32. Wang F, Zhao QH, Liu JZ, Kong DL. MiRNA-188-5p alleviates the progression of osteosarcoma via target degrading CCNT2. Eur Rev Med Pharmacol Sci. 2020; 24:29–35.
https://doi.org/10.26355/eurrev_202001_19892
PMID:31957815

33. Shi YK, Guo YH. MiR-139-5p suppresses osteosarcoma cell growth and invasion through regulating DNMT1. Biochem Biophys Res Commun. 2018; 503:459–66.
https://doi.org/10.1016/j.bbrc.2018.04.124
PMID:29673587

34. Mao C, Wang X, Liu Y, Wang M, Yan B, Jiang Y, Shi Y, Shen Y, Liu X, Lai W, Yang R, Xiao D, Cheng Y, et al. A G3BP1-Interacting lncRNA Promotes Ferroptosis and Apoptosis in Cancer via Nuclear Sequestration of p53. Cancer Res. 2018; 78:3484–96.
https://doi.org/10.1158/0008-5472.CAN-17-3454
PMID:29588351

SUPPLEMENTARY MATERIALS

Supplementary Figure

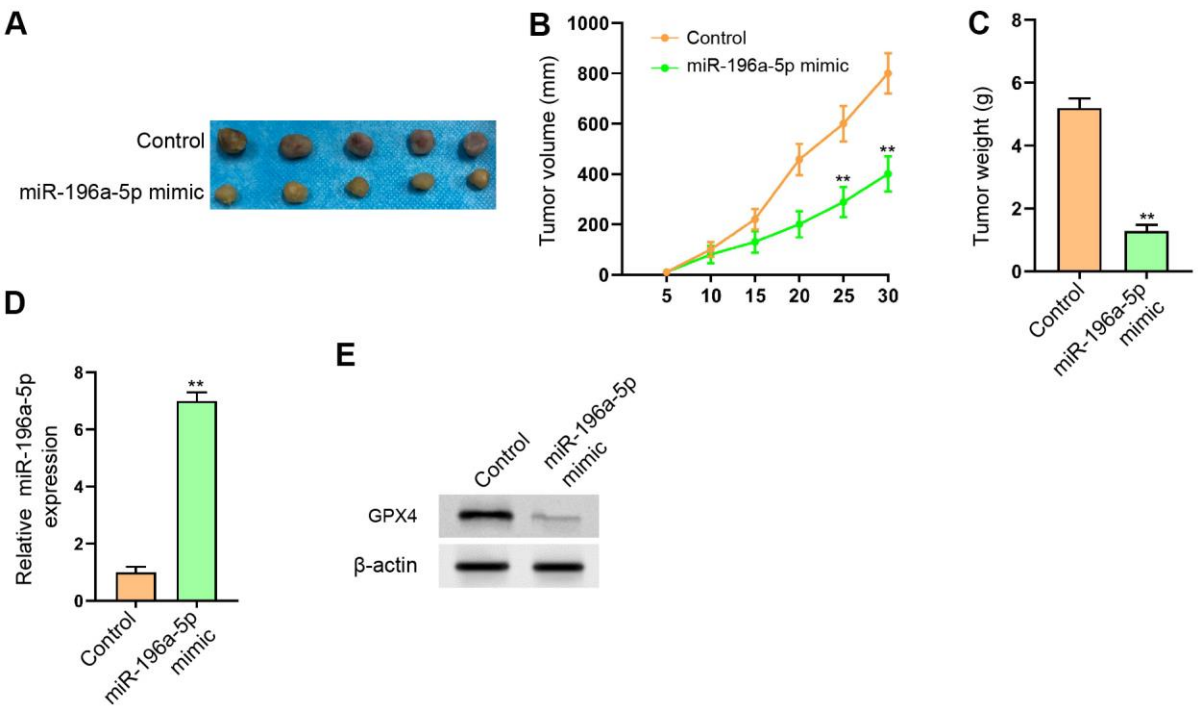

Supplementary Figure 1. MiR-196a-5p represses tumor growth of osteosarcoma *in vivo*. (**A**–**E**) Tumorigenicity assay in the nude mice (n = 5) analyzed the tumor growth of U2OS cells treated with miR-196a-5p mimic. The tumor images (**A**), tumor volume (**B**), and weight (**C**) were presented. (**D**) The qPCR detected miR-196a-5p expression in the tumor tissues. (**E**) Western blot analysis determined GPX4 expression in the tumor tissues. ** $P < 0.01$.